Austenite Grain Growth Kinetics in Al-Killed Plain Carbon Steels

MATTHIAS MILITZER, ALAN GIUMELLI, E. BRUCE HAWBOLT, and T. RAY MEADOWCROFT

Austenite grain growth kinetics have been investigated in three Al-killed plain carbon steels. Experimental results have been validated using the statistical grain growth model by Abbruzzese and Lücke, which takes pinning by second-phase particles into account. It is shown that the pinning force is a function of the pre-heat-treatment schedule. Extrapolation to the conditions of a hot-strip mill indicates that grain growth occurs without pinning during conventional processing. Analytical relations are proposed to simulate austenite grain growth for Al-killed plain carbon steels for any thermal path in a hot-strip mill.

I. INTRODUCTION

DURING the past 2 decades, microstructure engineering in hot-strip mills has gained significant attention with the goal being to develop a predictive tool that quantitatively links the processing parameters in the mill to the properties of the hot-rolled steel product. When hot rolling plain carbon steel, austenite grain growth is the dominant process in both the reheating furnace and between rolling stands after completion of recrystallization. The austenite microstructure after rolling and the cooling conditions on the runout table determine the final ferrite grain size and the associated mechanical properties, *e.g.*, strength and toughness of low-carbon steels.

To obtain the required quantitative link between process parameters and the resulting grain size, numerous studies of austenite grain growth kinetics have been performed and empirical relations have been proposed.[1–4] However, the extrapolation of these empirical relations to industrial conditions remains questionable because the thermomechanical treatment employed in an experiment is usually considerably different from the mill situation. Gladman and Pickering[5] revealed that AlN precipitation may strongly affect the austenite grain growth kinetics in Al-killed plain carbon steels. Because precipitation kinetics is a function of the thermomechanical path, the associated pinning force and, hence, grain growth, may depend on the pretreatment. This is similar to the findings of Drolet and Galibois[6] in Pb and Pb-Sn alloys, where it was found that preannealing alters the grain growth kinetics considerably. Moreover, empirical relations are usually based on grain-size measurements of two-dimensional (2-D) microstructures, virtually neglecting the three-dimensional (3-D) character of the grains. In fact, it is important to determine the actual volumetric grain size from the 2-D measurement and to explore the mechanisms of the experimentally observed grain-size evolution. With this information, it should be possible, using a model based on these mechanisms, to extrapolate to mill conditions.

The present article examines austenite grain growth kinetics in Al-killed plain carbon steels and develops an improved description of this process. The methods of Takayama *et al.*[7] and Matsuura and Itoh[8] are employed to estimate the 3-D grain-size distributions from the measured 2-D distributions. Austenite grain growth kinetics are described in terms of the statistical grain growth model of Abbruzzese and Lücke.[9] In this grain growth model, a pinning parameter is determined and extrapolated to describe grain growth during the delay between rough and finish rolling in the mill.

II. EXPERIMENTAL MATERIAL AND METHODOLOGY

Two commercial plain carbon steels, A36 and DQSK, received from the Gary Works of US Steel (Gary, Indiana) were investigated. In addition, experimental results from a third steel, 1080, which were obtained in a previous study,[10] are included in the analysis. The chemical compositions (wt pct) of the three steels are listed in Table I.

All tests on the A36 steel employed the Gleeble 1500 thermomechanical simulator using tubular specimens with a length of 20 mm, an inner diameter of 6 mm, and a wall thickness of 2 mm. This specimen design permits a statistically relevant number of grains across the thickness and minimizes the through-thickness thermal gradient during rapid cooling. The test samples were machined from an as-received transfer bar supplied by US Steel.

The following austenite grain growth tests were performed on the A36 steel.

(1) Isothermal tests at 950 °C, 1000 °C, 1050 °C, 1100 °C, and 1150 °C, with heating at 5 °C/s from room to the holding temperature.
(2) Stepped isothermal tests which involved heating the sample to 900 °C at 5 °C/s, holding for 120 seconds and rapidly heating (100 °C/s) to and holding at 1050 °C and 1100 °C.
(3) Soaking the test samples at 1200 °C for 3 hours in a sealed quartz tube followed by breaking the contain-

MATTHIAS MILITZER, Research Associate, and E. BRUCE HAWBOLT and T. RAY MEADOWCROFT, Professors, are with The Centre for Metallurgical Process Engineering, The University of British Columbia, Vancouver, BC, Canada V6T 1Z4. ALAN GIUMELLI, formerly Graduate Student, The Centre for Metallurgical Process Engineering, The University of British Columbia, is Development Engineer with the Hot Strip Mill, BHP Steel, Port Kembla, Wollongong 2500, Australia.

Manuscript submitted October 5, 1995.

Table I. Chemical Composition of the Steels (Weight Percent)

Steel	C	Mn	P	S	Si	Cu	Ni	Cr	Al	N
DQSK	0.038	0.30	0.010	0.008	0.009	0.015	0.025	0.033	0.040	0.0052
A36	0.17	0.74	0.009	0.008	0.012	0.016	0.010	0.019	0.040	0.0047
1080	0.78	0.68	0.024	0.014	0.025	NR*	NR*	NR*	0.035	NR*

*NR: not reported.

ment tube during water quenching. These samples were then isothermally tested at 950 °C with an initial heating rate of 300 °C/s.

(4) Tests to compare soaked and as-received steel by heating both at 50 °C/s to 950 °C, 1050 °C, and 1150 °C, where they were held for 2 minutes.

(5) A continuous cooling test that involved heating the as-received sample to 900 °C at 5 °C/s, holding for 120 seconds, and rapidly heating (100 °C/s) to 1120 °C, then cooling at 2 °C/s to temperatures ranging from 1100 °C to 1000 °C to simulate the delay between rough and finish rolling.

After each heat treatment, the specimens were quenched so as to retain the detail of the austenite microstructure and to allow identification of the prior austenite grain boundaries. Two quench regimes were employed. For larger grain sizes, above 35 μm, the samples were He quenched. By regulating the flow rate of the He gas, a ferrite fraction of approximately 5 pct was obtained, outlining the austenite boundaries. For smaller grain sizes, the samples were quenched more rapidly with water to obtain a martensitic microstructure in which the austenite boundaries were revealed by etching.[11]

To obtain detail of the austenite microstructure in the DQSK steel, an iced-brine quench was usually required. For this reason, austenite grain growth tests on this grade had to be performed in a vertical tube furnace that permitted a rapid downward quench into the iced brine. Variation of the pre-heat-treatment history is very limited under these conditions. Therefore, only isothermal tests at 1000 °C, 1050 °C, 1100 °C, and 1150 °C were performed. Sheet samples with a length of 25 mm, a width of 15 mm, and a thickness of 1.5 mm (3 mm for tests at 1150 °C) were machined from the as-received transfer bar material. The thicker samples were employed at 1150 °C to ensure at least 10-grain diameters across the thickness. The thin samples were used to obtain the higher quench rates required for revealing the finer grained austenite microstructures obtained after tests at lower temperatures. Depending on the specimen geometry, average heating rates of approximately 2 to 3 °C/s were attained on the thermocouple instrumented samples heated in the tube furnace.

The resulting grain-size distribution was measured with the C●IMAGING LC* Image Analysis System. The ASTM standard grain-size measurements[12] were performed manually, employing the linear intercept method (Heyn procedure), yielding the mean linear intercept l, as well as the area method (Jeffries procedure), yielding the mean area A, from which the equivalent area diameter (EQAD) d_A, is defined by

$$d_A = \sqrt{\frac{4A}{\pi}} \qquad [1]$$

In the previously investigated 1080 steel, the isothermal austenite grain growth kinetics were measured after a standard furnace treatment for temperatures ranging from 850 °C to 1150 °C. The grain size was quantified in terms of the EQAD by Jeffries method.[12]

*C●IMAGING LC is a trademark of Compix, Inc., Cranberry Township, PA.

III. CONSTRUCTION OF THE SPATIAL DISTRIBUTION

All of the grain-size measurements are obtained from a 2-D surface of a 3-D sample. Thus, the results do not give the spatial grain-size distribution, which is required for quantifying the volumetric grain size. Since it is very time consuming to determine the latter directly, a number of attempts have been made to construct the spatial distribution from 2-D measurements. In general, the early attempts assumed a spherical grain shape, which does not allow for space filling.[13,14] As a consequence, some doubtful results, *e.g.*, the predicted frequency of certain grain sizes dropping below zero, were obtained for the spatial distribution constructed in this way. However, Takayama *et al.*[7] have recently proposed a method to evaluate the spatial distribution from the 2-D standard measurements, assuming that the spatial distribution is log normal and the grain shape is that of a tetrakaidecahedron. The latter allows for space filling, whereas the former is characteristic for normal grain growth. Employing this method, first the log normality of the grain-size distribution has to be confirmed with measurements of the 2-D distribution, *e.g.*, as obtained from area measurements from an image analyzer. Then, the mean linear intercept l and mean area A are determined according to standard methods.[12]

The log normal distribution[15]

$$f(d) = \frac{1}{(2\pi s^2)^{1/2}\, d} \exp\left(\frac{-[\ln (d/d_g)]^2}{2s^2}\right) \qquad [2]$$

is characterized by the median grain size d_g and the standard deviation s. These parameters are related to the measured l and A according to Takayama *et al.*[7] by

$$l = 0.60661 d_g \exp (5s^2/2) \qquad [3]$$

and

$$A = 0.4861 d_g^2 \exp (4s^2) \qquad [4]$$

Thus, the measurement of l and A provides the required information to construct the spatial distribution using Eqs. [3] and [4]. Further, the average grain size of the 3-D log normal distribution is given by

$$d_m = d_g \exp (s^2/2) \qquad [5]$$

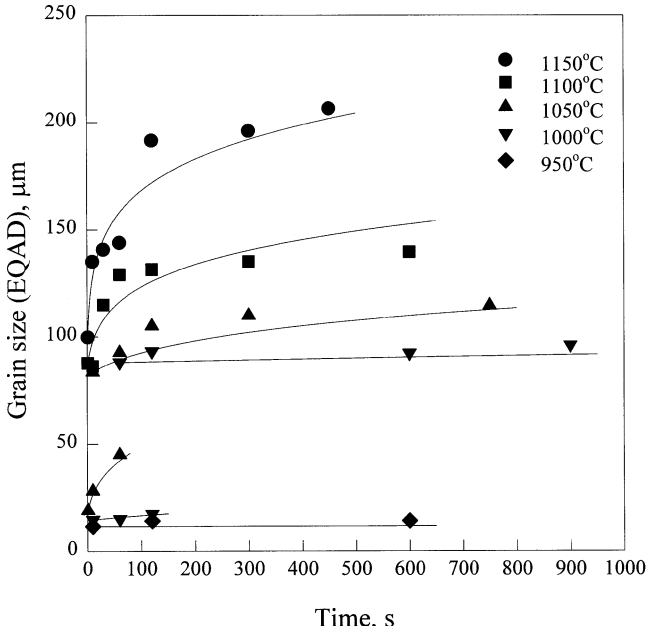

Fig. 1—Austenite grain growth kinetics in A36 steel after heating at ϕ = 5 °C/s to the isothermal measurement temperature. The experimental results and the lines representing the fit to Eq. [8] are shown.

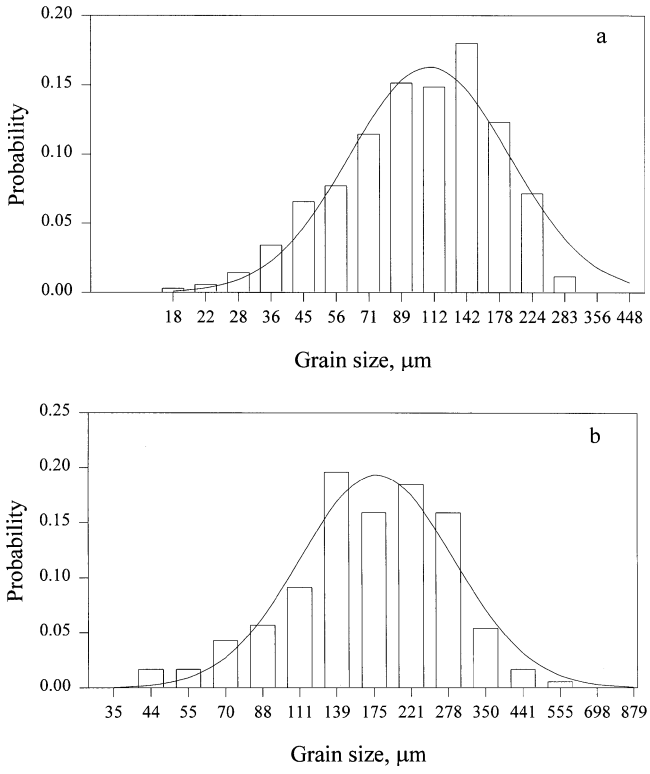

Fig. 2—Comparison of log normal distribution (solid lines) with experimental 2-D austenite grain size distribution in A36 steel at 1150 °C after (*a*) 60 s and (*b*) 450 s.

and the mean volumetric grain size by

$$d_V = d_g \exp(3s^2/2) \quad [6]$$

The mean volumetric grain size is the relevant grain size, since it actually represents the diameter of a grain with the average grain volume.

Although Takayama *et al.*[7] proposed a very convenient procedure to obtain the spatial grain-size distribution, it should be emphasized that their method can only be applied when the grain-size distribution is log normal, *i.e.*, for normal grain growth. Matsuura and Itoh[8] proposed a more general method to construct the 3-D distribution, which also allows for deviations from the log normality. Twelve types of polyhedra are employed in this method to describe the variety of grain shapes in the actual material; no additional assumptions are made. The 3-D distribution can then be calculated from the 2-D measurements with the help of a sophisticated computer code. Both methods were employed to estimate the 3-D grain-size distribution, with similar results.

IV. EXPERIMENTAL RESULTS

A. *Grain Growth in A36 Steel*

For each test, the number of grains measured is in the range 200 to 500. The average experimental error in determining l and A is approximately 10 pct. Figure 1 shows the results of isothermal grain growth when the heating rate to the measurement temperature ϕ is 5 °C/s. The initial EQAD is approximately 15 μm for $T < 1050$ °C and above 80 μm for $T \geq 1050$ °C, indicative of substantial grain growth occurring during heating to the higher temperatures. This rapid grain coarsening can presumably be attributed to abnormal growth processes, which are related to coarsening and dissolution of AlN particles. Abnormal growth is observed in the range 950 °C to 1050 °C; for a holding time decreasing from 600 seconds at 950 °C to 10 seconds at 1050 °C, a nonhomogeneous microstructure develops in which areas of fine grains are embedded in regions of substantially larger grains. The fine grain areas eventually disappear and normal growth of the coarser grains takes place.

A comparison of the log normal distribution and the experimental 2-D grain size distribution is shown in Figure 2 for holding times of 60 and 450 seconds at 1150 °C. The results support the log normality of the distribution, which is characteristic of normal grain growth. Figure 3 shows the grain growth kinetics for the stepped isothermal tests employing rapid heating from 900 °C to the measurement temperature. This stepped-heat-treatment procedure significantly reduces the effects of abnormal grain growth. A nonhomogeneous microstructure is initially observed, but disappears after a few seconds. The initial EQAD of the larger grains is approximately 50 μm, and normal growth of these grains is observed. For both slow and fast heating rates, a limiting grain size is approached after approximately 120 seconds. The limiting grain size obtained for the slower heating rate is substantially larger than that obtained for the rapid heating tests, as illustrated in Figure 4 for austenite grain growth at 1100 °C. The limiting EQAD for the tests performed at 1100 °C decreases from 140 μm at a heating rate of 5 °C/s to 100 μm obtained at 100 °C/s. Similar tests performed at 1050 °C showed that the limiting EQAD decreased from 115 μm for 5 °C/s to 85 μm for 100 °C/s.

Wilson and Gladman[16] and Kunze[17] critically evaluated the wide variety of AlN solubility products proposed in the literature. Wilson and Gladman concluded that for practical heat-treatment purposes, the solubility of AlN can be rep-

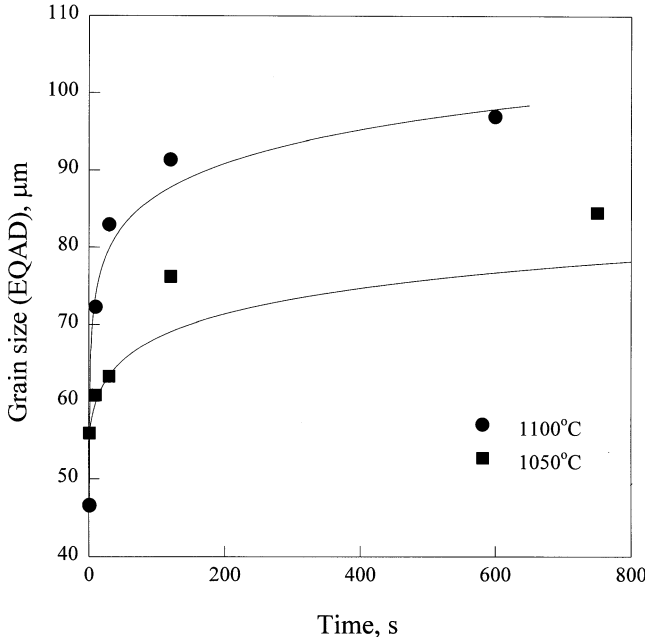

Fig. 3—Austenite isothermal grain growth kinetics in the A36 steel obtained after heating at ϕ = 100 °C/s from the austenitizing temperature of 900 °C to the designated measurement temperature. The experimental results and the lines representing the fit based on Eq. [8] are shown.

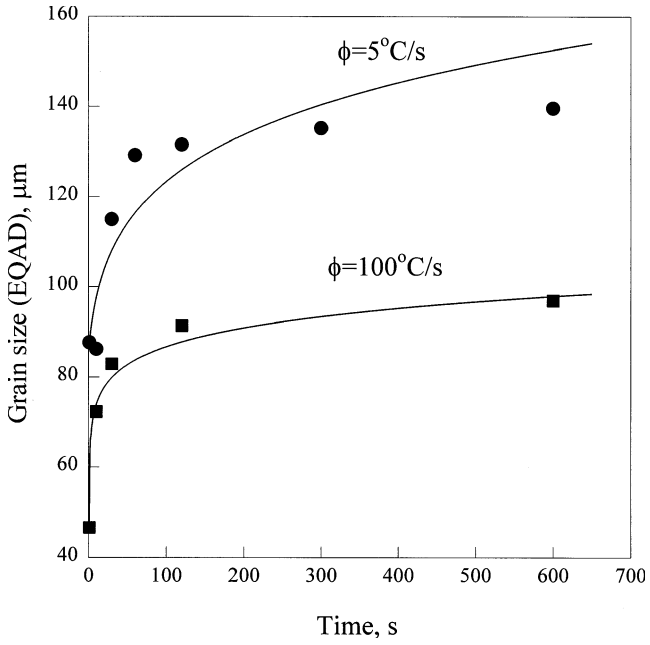

Fig. 4—Comparison of austenite grain growth at 1100 °C in the as-received A36 steel after heating at different rates, ϕ. The experimental results and the lines representing the fit based on Eq. [8] are shown.

resented by[18]

$$\log [Al][N] = -6770/T + 1.03 \qquad [7a]$$

where the concentrations [Al] and [N] are in wt pct. By including the effects of alloying elements on the N solubility, Kunze later proposed

$$\log [Al][N] = -7261/T + 1.553 \qquad [7b]$$

Employing Eqs. [7a] and [7b], the solubility temperature of

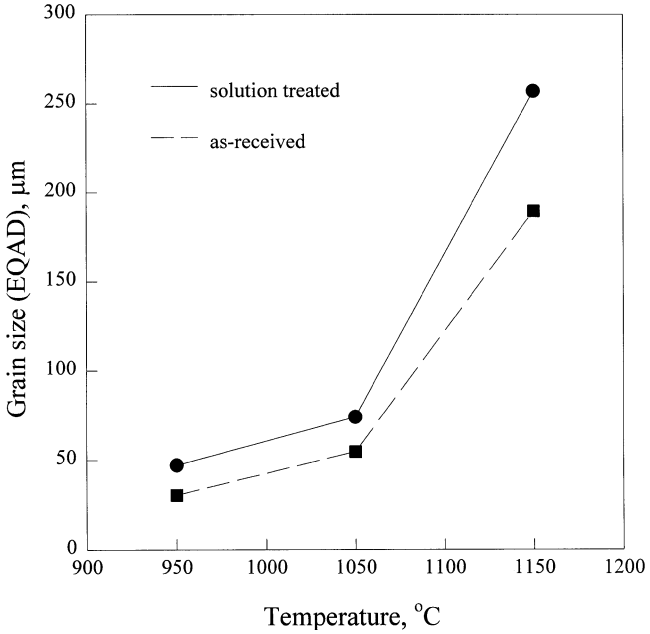

Fig. 5—Comparison of the austenite grain size attained after heating at 50 °C/s to the test temperature and holding for 2 min for the as-received and the solution-treated A36 steel.

AlN in the A36 steel is estimated to be 1100 °C to 1150 °C. Thus, to eliminate the effect of AlN precipitation, the as-received material was soaked for 3 hours at 1200 °C (solution treated) to completely dissolve the AlN particles. To reduce reprecipitation during cooling to room temperature, the samples were water quenched after soaking. To minimize reprecipitation during heating, high heating rates in the range 50 to 300 °C/s were employed. The grain growth in the soaked samples at 950 °C had a substantially higher growth rate than observed for the as-received material, even though the latter was heated at the slower heating rate of 5 °C/s to 950 °C/s. In the solution-treated samples, the EQAD increases from 31 to 36 μm after 10 minutes, whereas in the as-received material, growth from 12.5 to 15 μm is observed during the same holding time. To clearly separate the effect of the soaking heat treatment on grain growth, solution-treated and as-received samples were subjected to the same grain growth tests; these consisted of heating at 50 °C/s to the measurement temperature and holding for 2 minutes. The results, as shown in Figure 5, confirm the expected larger austenite grain size for the soaked specimens as a result of a significantly reduced AlN precipitation. The results also display the characteristically higher growth rates obtained at higher temperatures (≥1050 °C). This is indicative of some reprecipitation of AlN in the solution-treated samples during holding at lower temperatures.

The experimental data in Figures 1, 3, and 4 have been described using the conventional empirical power law

$$d_A^m = d_{A.0}^m + K_o \exp(-Q/RT)t \qquad [8]$$

where the growth exponent m, the apparent activation energy Q, and K_o are the fitting parameters. Table II summarizes values obtained for these parameters for the lines shown in Figures 1, 3, and 4. It is obvious that the isothermal grain growth rates depend strongly on the preheat

Table II. Empirical Parameters for the Grain Growth Power Law in the As-Received A36 Steel

Series	m	Q/kJ mol^{-1}	$K_o/\mu m^m$ s^{-1}
ϕ = 5 °C/s (fine grains)	3.4	1291	5.46×10^{54}
ϕ = 5 °C/s (coarse grains)	8.2	840	1.51×10^{47}
ϕ = 100 °C/s	14.9	1089	1.94×10^{68}

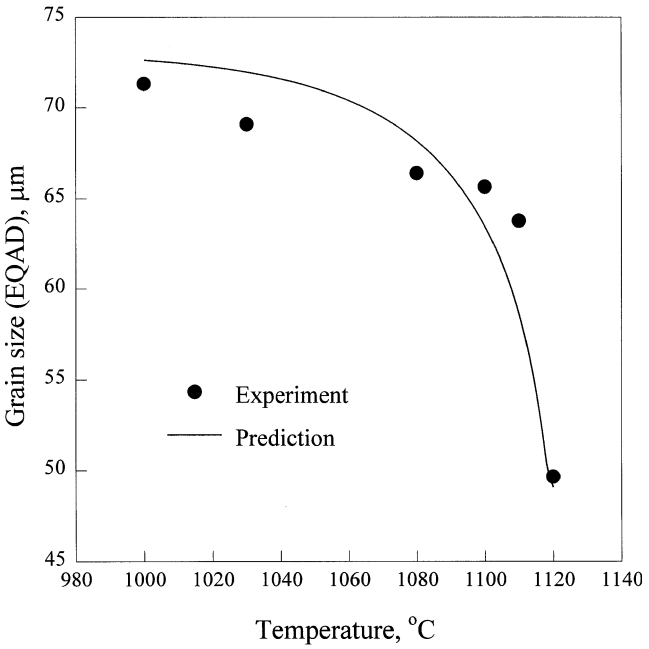

Fig. 6—Austenite grain growth kinetics in the A36 steel during continuous cooling from 1120 °C to 1000 °C at 2 °C/s. The solid line represents the prediction from the statistical grain growth model with the pinning parameter described in Eq. [17].

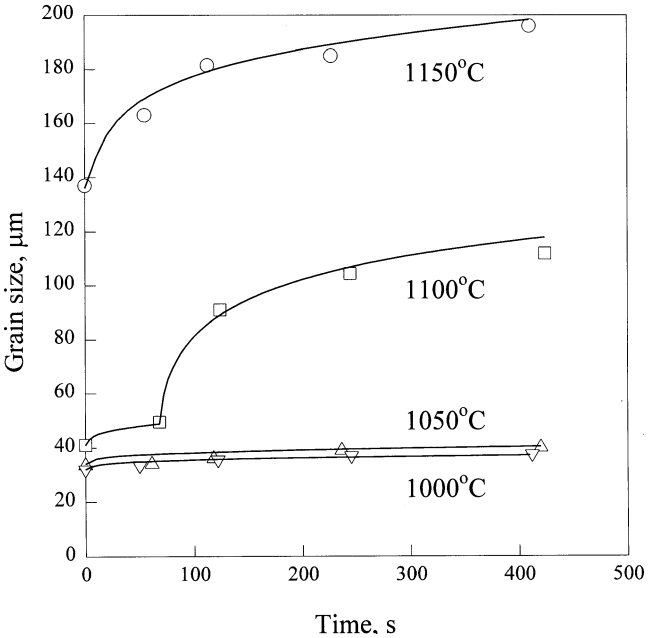

Fig. 7—Comparison of the isothermal grain growth kinetics in the DQSK steel with the predictions from the statistical grain growth model (solid lines). The grain size is represented by the average value, d_m, according to Eqs. [5] and [9c].

treatment history, which determines the size and volume fraction of AlN precipitates. This effect seriously limits the validity of using an empirical power law to describe austenite grain growth.

In the continuous-cooling test designed to simulate the delay between rough and finish rolling, no evidence of abnormal grain growth was observed, presumably due to the somewhat higher initial temperature of 1120 °C, where the initial EQAD is approximately 50 μm. Initial rapid grain growth occurs at the higher temperatures but the growth rate quickly decreases with increasing growth time, as illustrated in Figure 6. The EQAD at 1000 °C is 71 μm. This is a substantially smaller grain size than is obtained under mill conditions, where an EQAD of approximately 160 μm is observed, despite the fact that the initial EQAD of 50 μm is in the range readily expected for the grain size of recrystallized austenite after rough rolling.

Since the grain-size distribution is log normal for normal grain growth (Figure 2), Takayama's[7] method to determine the spatial distribution is applicable for austenite grain growth at the higher temperatures of interest. Because the standard deviation s is sensitive to the ratio l^2/A, experimental errors in l and A can produce large scatter in s. However, the mean value of s for each isothermal test is approximately 0.3. Thus $s = 0.3$ is employed to estimate the spatial distribution, which is, to a first approximation, equivalent to the following relations between the measured values and the mean volumetric diameter.

$$d_V = 1.5l \quad [9a]$$

$$d_V = 1.2d_A \quad [9b]$$

$$d_m = 1.1d_A \quad [9c]$$

It is worth noting that an assessment of the spatial distribution obtained from the more general, but more sophisticated, Matsuura–Itoh method indicates similar conversion factors to those given in the preceding relations.

B. *Grain Growth in the DQSK Steel and the 1080 Steel*

Figure 7 shows the results of grain growth tests in the DQSK steel. The growth behavior follows similar patterns to those observed in the A36 steel. At low temperatures (1000 °C and 1050 °C), very little growth is observed and the limiting EQAD remains below 40 μm. At 1100 °C, the austenite grains are initially strongly pinned, even after holding for approximately 1 minute. Thereafter, rapid grain growth develops *via* a short period of abnormal growth. At a higher temperature (1150 °C), this abnormal growth period has taken place during heating, and normal growth takes place starting from a high initial EQAD of approximately 140 μm. The estimation of the 3-D distribution employing the Matsuura–Itoh method gives results similar to those obtained for the A36 steel, *i.e.*, a distribution width s of approximately 0.3 can also be adopted for normal growth in the DQSK steel.

Previous grain growth studies[10] show an apparently more gradual increase of the coarsening rate with temperature in the 1080 steel (Figure 8). However, the increasing initial grain size with temperature indicates that rapid growth during heating above approximately 1000 °C has been taken place. The similarity of grain growth kinetics in all grades can be attributed to the fact that they are Al-killed steels. It would appear, therefore, that AlN precipi-

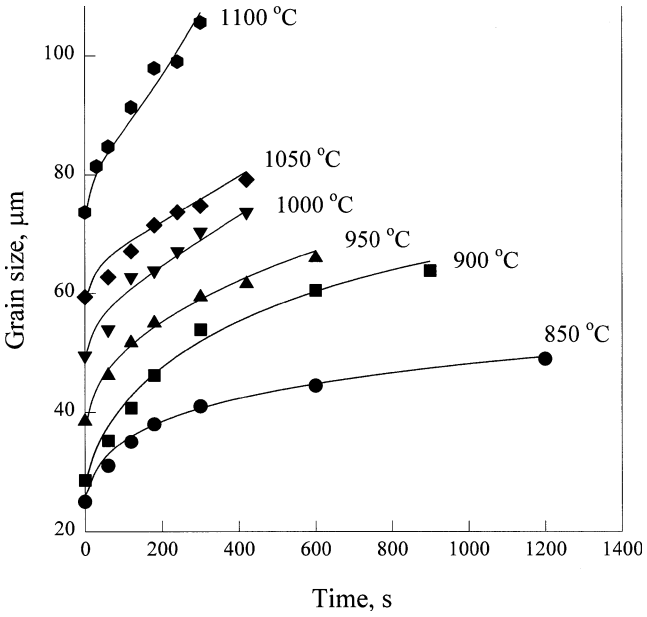

Fig. 8—Comparison of the isothermal grain growth kinetics in the 1080 steel with predictions from the statistical grain growth model (solid lines). The grain size is represented by the average value, d_m, according to Eqs. [5] and [9c].

tation markedly affects the austenite grain growth kinetics in all three steels. A more detailed comparison of the observed grain growth in these three steels appears to be of limited use because of the different pre-heat-treatment histories employed for each steel.

V. MODELING

A. *Statistical Grain Growth Model*

The statistical grain growth model of Abbruzzese and Lücke[9] can be employed to predict grain growth kinetics. In this approach, a pinning parameter accounts for the characteristic inhibition of normal grain growth due to precipitates and solute drag. The basic assumptions and equations of the model follow. The actual grain structure is replaced by a spherical grain structure with equal grain volume. The grain-size distribution $f(R)$ can be subdivided logarithmically into n grain-size classes. Then, growth or shrinkage of a grain of size class i (grain radius R_i) is considered under the assumption that it is surrounded statistically by grains of all other size classes. Provided size i is sufficiently greater than size j, a driving force $F_{ij} > 0$ exists and grain i tends to consume neighboring grain j, where

$$F_{ij} = \gamma_{gb}\left(\frac{1}{R_j} - \frac{1}{R_i} - P\right) \qquad [10]$$

Here, γ_{gb} is the grain-boundary energy and P is related to the pinning force F_P by $P = F_P/\gamma_{gb}$. The following relationships hold for the driving forces: $F_{ij} = -F_{ji}$ and $F_{ij} = 0$ if $F_{ij} < 0$ for $R_i > R_j$. The growth (or shrinkage) rate of a grain with size i is

$$\frac{dR_i}{dt} = M_{gb}\sum_j w_{ij}F_{ij} \qquad [11]$$

The grain-boundary mobility M_{gb} is approximated with the grain-boundary diffusion D_{gb} by

$$M_{gb} = D_{gb}b^2/\mathrm{k}T \qquad [12]$$

where b is the magnitude of the Burgers vector. The probability w_{ij} that grains i and j are neighbors, is given for a random distribution by

$$w_{ij} = \frac{f_jR_j^2}{\sum_j f_jR_j^2} \qquad [13]$$

where $f_j = N_j/N_{\mathrm{tot}}$ represents the fraction of grains with size j. Here, N_j is the number of grains per unit volume in class j and N_{tot} is the total number of grains per unit volume. The change in the grain size distribution can then be calculated per time-step from

$$\frac{df_i}{dt} = \frac{1}{\ln\alpha}\left[\frac{f_{i+1}}{R_{i+1}}\left|\frac{dR_{i+1}}{dt}\right|\Theta\left(-\frac{dR_{i+1}}{dt}\right) + \frac{f_{i-1}}{R_{i-1}}\frac{dR_{i-1}}{dt}\Theta\left(\frac{dR_{i-1}}{dt}\right) - \frac{f_i}{R_i}\left|\frac{dR_i}{dt}\right|\right] \qquad [14]$$

where α is the geometrical multiplying factor characterizing the size-class width in a logarithmic scale and $\Theta(x)$ is the step function, with $\Theta(x) = 1$ for $x > 0$ and $\Theta(x) = 0$ for $x \le 0$. Following this procedure, the grain-size evolution is predicted. The model was further extended to account for nonisothermal conditions.

B. *Prediction of the Pinning Force*

This model can be applied to the grain growth kinetics in the three plain carbon steels. Grain-boundary energy has been determined by Gjostein *et al.*[19] to decrease with carbon content because of increasing carbon grain-boundary segregation. According to these findings,

$$\gamma_{gb} = (0.8 - 0.35C^{0.68}) \qquad (\text{in J m}^{-2}) \qquad [15]$$

can approximately be written where C is the carbon concentration in wt pct with $C \le 0.8$. Consequently, $\gamma_{gb} = 0.7$ J m^{-2} is employed for the A36 steel, $\gamma_{gb} = 0.8$ J m^{-2} for the DQSK steel, and $\gamma_{gb} = 0.5$ J m^{-2} for the 1080 steel. The grain-boundary mobility M_{gb} is, to a first approximation, assumed to be independent of composition for plain carbon steels and is estimated from the parameters of pure Fe, *i.e.*, $D_{gb} = 0.89$ cm^2 s^{-1} exp (-1.66 eV/kT) and $b = 2.58$ Å.[20]

Using P as a fitting parameter, good agreement with the experimental results has been achieved, as shown by the solid lines in Figures 7 through 9. The pinning parameter decreases with temperature, as illustrated in Figures 10 through 12. Furthermore, the pinning parameter increases with increasing heating rate in the as-received A36 steel. At high temperatures (≥1050 °C) when normal grain growth occurs, a linear decrease of P with temperature (in °C) is confirmed for $\phi = 5$ °C/s, where

$$P = -75(T - 1251) \qquad (\text{in m}^{-1}) \qquad [16]$$

and for $\phi = 100$ °C/s,

$$P = -80(T - 1313) \qquad (\text{in m}^{-1}) \qquad [17]$$

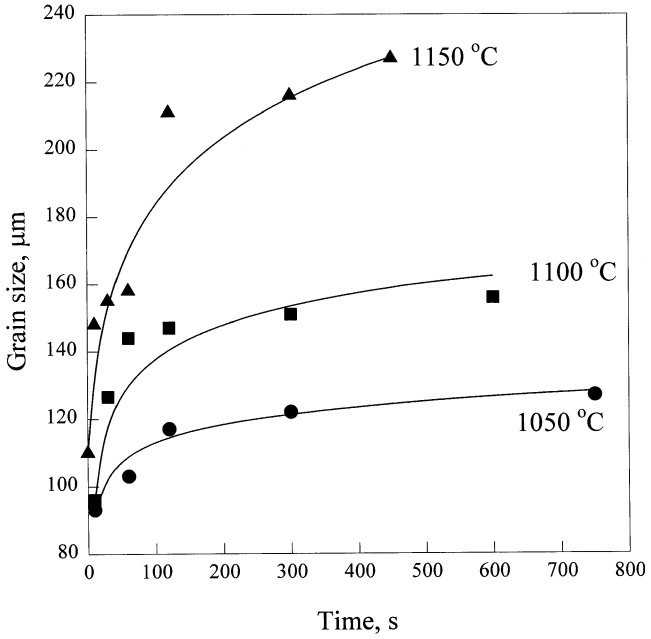

Fig. 9—Comparison of the predictions from the statistical grain growth model (solid lines) with austenite isothermal grain growth kinetics in the A36 steel occurring by normal growth for an initial heating rate, $\phi = 5$ °C/s. The grain size is represented by the average value, d_m, according to Eqs. [5] and [9c].

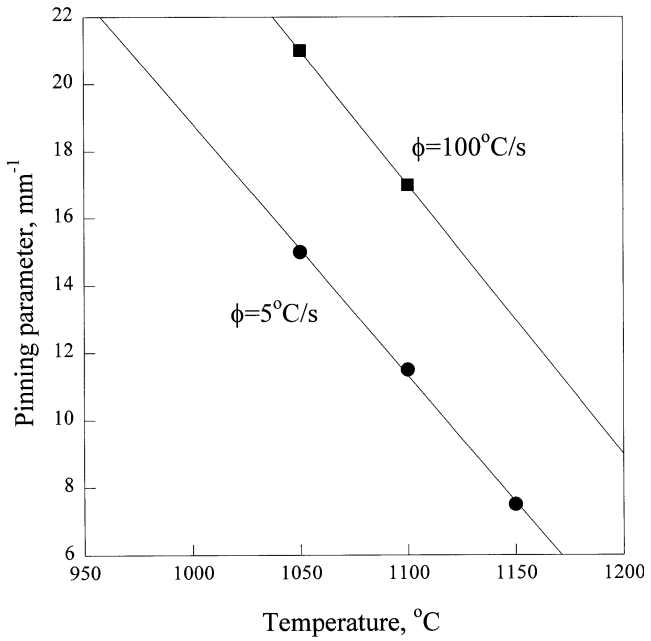

Fig. 10—Pinning parameter for the as-received A36 steel as a function of temperature for different heating rates, ϕ.

is obtained. Moreover, the pinning parameter depends markedly on the soaking treatment; at 950 °C after heating at 300 °C/s, $P = 45$ mm^{-1} is obtained for the soaked A36 specimens, which is approximately one-third of the value for the as-received material ($P = 140$ mm^{-1}). The abnormal growth in the DQSK steel at 1100 °C has been simulated assuming a high pinning force for initial growth and a significantly lower pinning force for the second growth stage, which occurs after approximately 1 minute holding time. This reflects the transition from strongly pinned growth at

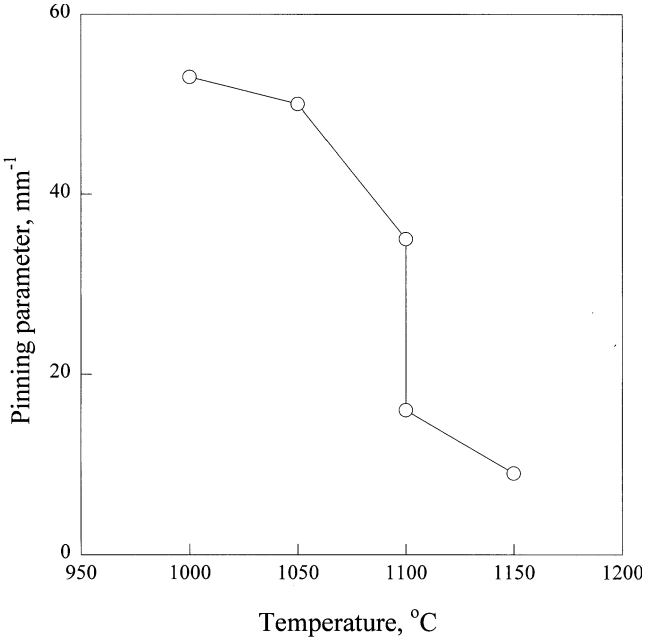

Fig. 11—Pinning parameter for the as-received DQSK steel.

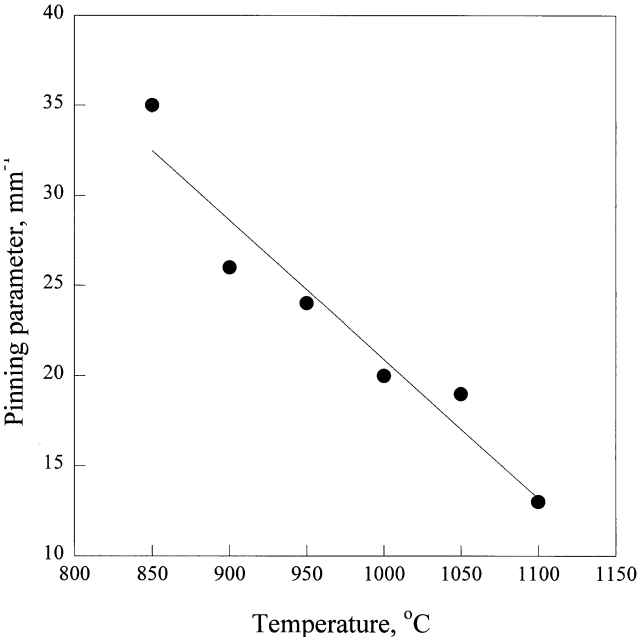

Fig. 12—Pinning parameter for the 1080 steel.

a lower temperature ($P > 40$ mm^{-1}) to reduced pinning at a higher temperature ($P < 20$ mm^{-1}) consistent with the experimental grain growth conditions. On the other hand, an approximately linear decrease of P with temperature is observed over the entire temperature range from 850 °C to 1100 °C in the 1080 steel, where

$$P = -77(T - 1273) \qquad (\text{in m}^{-1}) \qquad [18]$$

is obtained, similar to the high temperature A36 results.

Zener[21] proposed an expression for pinning related to the presence of particles as follows:

$$P = \frac{3\nu}{4r} \qquad [19]$$

where v is the volume fraction of particles and r the mean particle radius. Assuming that r for AlN is in the range 5 to 10 nm,[22] the predicted P corresponds to reasonable values of v in the range of 10^{-5} to 10^{-3}. As illustrated in Figure 13, P also compares favorably to Zener's criterion for the limiting grain radius

$$R_{\text{lim}} = P^{-1} \quad [20]$$

where the grain size, which is measured after the longest holding times for the A36 and the DQSK steels, can be taken as an indication of the limiting grain size.

Furthermore, the Abbruzzese–Lücke model[9] predicts a grain size distribution which becomes more narrow as the pinning force increases. Employing Takayama's method, an initial width $s_0 = 0.3$, consistent with the experimental results, is assumed for the grain-size distribution at low temperatures, before the onset of abnormal growth. At higher temperatures, where grain growth after abnormal growth is simulated, an initial width $s_0 \approx 0.4 - 0.45$ is taken to reflect the broadening of the distribution as a result of abnormal growth. However, for these cases, the width of the log normal distribution decreases rapidly with time to approximately 0.25 to 0.3 in accordance with the predicted values of P. Thus, the predictions of the Abbruzzese–Lücke model appear to be consistent with the estimation of the 3-D grain-size distributions in the lower carbon A36 and DQSK grades.

Unlike the lower carbon grades, austenite grain growth in the 1080 steel displays a more progressive linear decrease of the pinning force over the entire temperature range studied (Figure 12). Further, the initial grain size increases gradually with temperature and no limiting grain size has been attained during the tests, despite holding times comparable to those in the DQSK and the A36 steels. In fact, the final grain size obtained in the 1080 steel is approximately 90 pct of the limiting grain size at lower temperatures (≤900 °C), with this ratio decreasing to approximately 70 pct at 1100 °C. Interestingly, the increasing initial grain size and decreasing pinning force with temperature also is reflected in the calculations by assuming an initial width s_0 of the grain-size distribution, which decreases gradually from 0.4 at 850 °C to 0.25 at 1100 °C. This is consistent with the predicted sharpening of the distribution during grain growth with pinning, which takes place during the comparatively long heating period to the higher temperatures.

Figure 6 compares the model predictions of the Abbruzzese–Lücke model with the continuous-cooling test performed in the A36 steel. As shown by the solid line, the observed grain growth kinetics are consistent with the Abbruzzese–Lücke model, assuming the pinning parameter described by Eq. [17], which corresponds to that obtained for the stepped isothermal tests. Rapid grain growth takes place during the initial stages of cooling from 1120 °C, before the growth rate quickly decreases with decreasing temperature. An EQAD of 72 μm is predicted at 1000 °C, with the experimental value being 71 μm.

VI. AUSTENITE GRAIN GROWTH IN A HOT-STRIP MILL

The test results clearly indicate that the heat-treatment schedule, particularly the variation in heating rate ϕ, can have a considerable effect on the subsequent grain growth behavior. Such behavior can be attributed to variations of the volume fraction v and the radius r of the precipitates. Consequently, it is not surprising that the continuous-cooling test for the A36 steel, designed to simulate the grain growth obtained during the delay associated with the exit from the roughing mill and the entrance to the finishing mill, with a change of temperature from 1120 °C to 1000 °C at 2 °C/s, resulted in a much smaller grain size (EQAD 71 μm, Figure 6) than that observed under mill conditions (EQAD 160 μm). This difference can be attributed to the fact that in the simulation AlN is not dissolved, whereas it does go into solution in the mill. Preheating for the cooling test consisted of heating at 5 °C/s to 900 °C, holding for 120 seconds, then rapidly heating at 100 °C/s to 1120 °C, with no holding at this temperature; this treatment does not allow for substantial dissolution of AlN particles. In the mill, however, the material is reheated for several hours at approximately 1300 °C, allowing AlN particles to dissolve, followed by rough rolling above the solution temperature of AlN. Reprecipitation of AlN during cooling, a comparatively slow process,[16] is expected to take place in the A36 and other Al-killed plain carbon steels below 1000 °C. Thus, austenite grain growth during the rougher to finisher delay in the mill is not inhibited by the presence of AlN, whereas in the experimental continuous cooling test, a significant number of AlN particles are expected to have survived the rapid heating.

Employing the Abbruzzese–Lücke model, the effective pinning parameter for delay in the mill (cooling from 1120 °C to 1000 °C in 60 seconds) was estimated. Taking the recrystallized grain size after roughing to be 50 to 100 μm, marginal pinning, *i.e.*, $P \approx 0$, is required to obtain the observed grain coarsening to an average grain size d_m of approximately 180 μm before finishing. This is indicative of unpinned austenite grain growth taking place in the Al-killed plain carbon steels when recrystallization is completed after each rough rolling pass.

Unpinned growth is described by[23]

$$\frac{d(d_m)}{dt} = \frac{K}{2d_m} \quad [21]$$

where the growth constant K can be expressed as a function of γ_{gb} and M_{gb}

$$K = 3\gamma_{gb}M_{gb} \quad [22]$$

As discussed previously, the grain-boundary energy γ_{gb} increases with decreasing carbon content according to Gjostein *et al.*,[19] whereas, at least for low-carbon steels, the grain-boundary mobility can be assumed to be that of pure Fe. Komatsubara *et al.*[24] reported that Mn segregation is expected to decrease the grain-boundary mobility. However, it is difficult to quantify this effect reliably. In an alternative way, it can effectively be included as a solute drag addition to the pinning parameter.

In the isothermal case, integration of Eq. [21] gives

$$d_m = \sqrt{d_{m,0}^2 + Kt} \quad [23]$$

the parabolic grain growth law, where $d_{m,0}$ is the initial grain size. Unpinned grain growth, according to Eq. [23], has also been confirmed by Monte Carlo simulations.[25] It should be emphasized that unpinned normal growth is as-

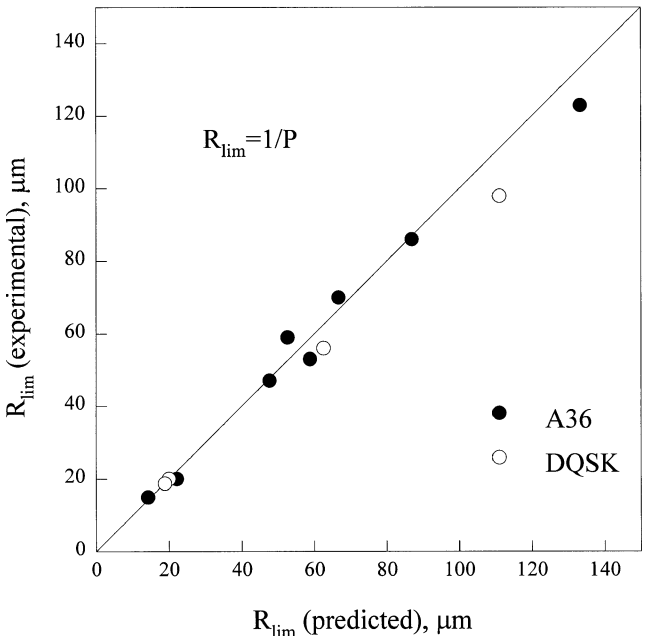

Fig. 13—Comparison of experimentally observed limiting grain radius and those predicted from the pinning parameter employing Zener's criterion.

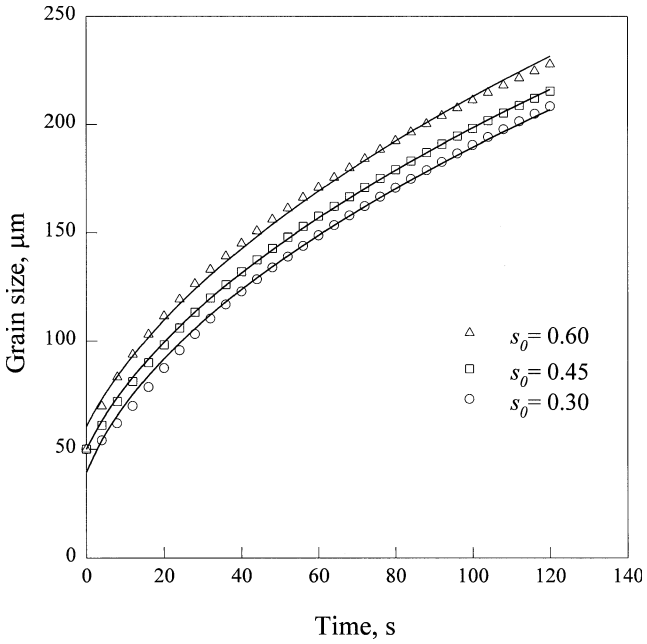

Fig. 14—Unpinned austenite grain growth at 1050 °C in the DQSK steel for different initial log normal distributions with $d_{m,0}$ = 50 μm. The symbols represent the results from the Abbruzzese–Lücke model; the solid lines give the fit to the parabolic growth law with a correction for initial growth.

sociated with a scaling log normal distribution where the width s is approximately 0.45.

When continuous cooling $T(t) = T(0) - \varphi t$ is considered, integration of Eq. [21] and using Eqs. [12] and [22] leads to

$$d_m = \sqrt{d_{m,0}^2 + \frac{3\gamma_{gb} b^2 D_{o,gb}}{\varphi k} \int_{Q_{gb}/kT(0)}^{Q_{gb}/kT(t)} \frac{e^{-x}}{x}\, dx} \qquad [24]$$

where $D_{o,gb}$ is the pre-exponential factor and Q_{gb} the activation energy of grain-boundary diffusion. For an arbitrary thermal history

$$d_m = \sqrt{d_{m,0}^2 + \frac{3\gamma_{gb} b^2 D_{o,gb}}{k} \int_{t_o}^{t} \frac{e^{-Q_{gb}/kT(t')}}{T(t')}\, dt'} \qquad [25]$$

can be written.

In the mill, the initial austenite grain-size distribution is normally not a result of grain growth but of the phase transformation from ferrite to austenite on reheating and of recrystallization during interpass times. Therefore, the initial grain-size distribution may be quite different from the scaling log normal distribution. The influence of a variation in the initial grain-size distribution on subsequent unpinned grain growth has been simulated with the Abbruzzese–Lücke model by assuming different initial widths s_0 of the log normal distribution. The results for isothermal grain growth at 1050 °C in the DQSK steel with $d_{m,0}$ = 50 μm are shown in Figure 14. With increasing s_0, the initial growth rate increases, but the grain-size distribution quickly attains its scaling shape, so that the grain growth rate reaches the values according to Eq. [21] after a short initial period. As indicated in Figure 14, this behavior can be accounted for by introducing an effective value for $d_{m,0}$; in the given case, the effective $d_{m,0}$ is approximately 40 μm for s_0 = 0.3, and has its actual value (50 μm) for s_0 = 0.45, the scaling distribution, and is approximately 60 μm for s_0 = 0.6 to reflect the higher initial growth rate associated with the wider initial size distribution. However, it should be noted that the effect is minor for typical growth times ≥30 seconds, *e.g.*, the grain sizes attained after 120 seconds are 208, 215, and 228 μm, respectively. This is also verified with a simulation of nonisothermal grain growth, in which the material is continuously cooled from 1120 °C to 1000 °C in 1 minute. The grain size at 1000 °C predicted from Eq. [24] is 160 μm for a grain size distribution s_0 = 0.45, which scales from the beginning. Assuming an initially wider (s_0 = 0.6) or smaller (s_0 = 0.3) distribution changes this grain size by less than 10 pct to 173 and 150 μm, respectively.

These results suggest that the shape of the initial grain-size distribution is of minor importance for grain growth during reheating, during the interpass times of rough rolling, and during the delay between rough and finish rolling. Consequently, Eq. [25] can be used to assess austenite grain growth in the mill above 1000 °C. Figure 15 shows the estimation of grain growth in the A36 and the DQSK steel during continuous cooling from 1120 °C to 1000 °C at 2 °C/s. The initial grain size is varied from 50 to 100 μm to cover the anticipated range of recrystallized grain sizes attained after rough rolling. The 50 μm difference in the initial grain size is reduced to approximately a 20 μm difference in the grain size at 1000 °C, *i.e.*, to approximately 10 pct of its absolute value. This further indicates that an exact knowledge of the initial grain size is of minor importance when sufficient time is available for normal grain growth to take place. Grain growth in the DQSK grade is expected to be slightly faster than that in the A36 steel because of the relatively higher driving force associated with the higher grain-boundary energy in the lower carbon grade.

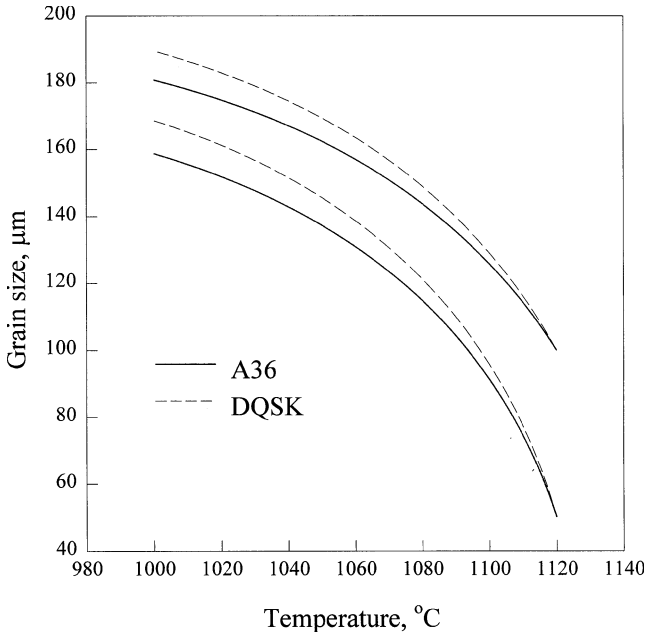

Fig. 15—Prediction of austenite grain growth in plain carbon steels during the delay between rough and finish rolling in a hot strip mill. The delay period is assumed to be characterized by cooling from 1120 °C to 1000 °C at 2 °C/s.

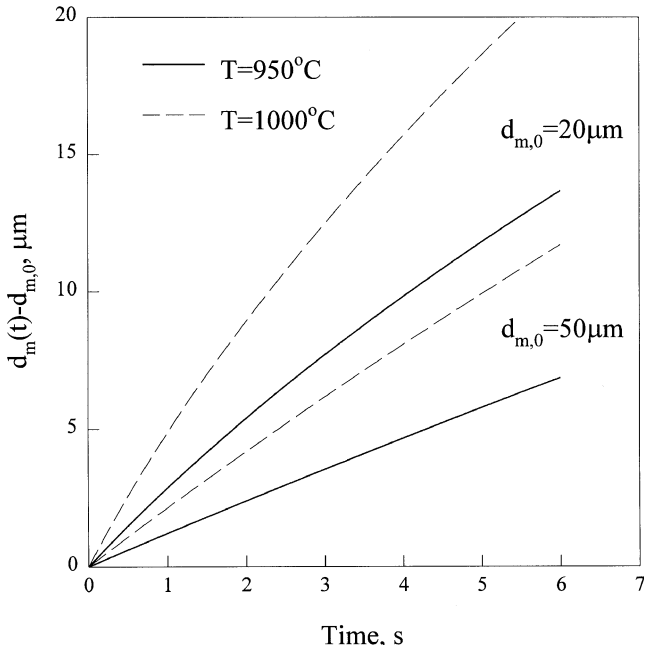

Fig. 16—Evaluation of austenite grain growth in the DQSK steel during finish mill interstand times after completion of recrystallization, where the recrystallized grain size represents the initial grain size, $d_{m,0}$.

During finish rolling with interstand times decreasing from a few seconds to a fraction of a second, grain growth after completion of recrystallization should be of minor importance. Grain growth under these conditions may be pinned because of strain-induced precipitation of AlN below 1000 °C. It should also depend strongly on the initial grain-size distribution, which is attained by recrystallization. Thus, Eqs. [23] through [25] can only be used as an approximation for the upper limit of possible grain growth during finish-mill conditions. An assessment of these upper limits is shown in Figure 16 for the DQSK steel. For 1 second at 1000 °C, grain coarsening of approximately 5 μm occurs when the recrystallized grain size is 20 μm, and 2 μm growth occurs for a recrystallized grain size of 50 μm. For 1 second at 950 °C, these growth values are reduced to approximately 2 μm and 1μm, respectively. For higher carbon grades, these numbers decrease slightly because of the somewhat smaller grain-boundary energy (Eq. 15). Therefore, actual grain growth after completion of recrystallization, during the short interstand times of the finishing mill, can readily be neglected for plain carbon steels. Thus, the grain size obtained during finish rolling can be described, in a first approximation, by the recrystallized grain size distribution.

In microalloyed grades, grain growth before finish rolling also may occur with pinning under mill conditions, particularly when the steel contains Ti, since TiN usually does not completely dissolve during reheating.[26] The Abbruzzese–Lücke model is recommended for simulating pinned grain growth; empirical relations found in conventional grain growth tests can only be used with extreme caution.

VII. CONCLUSIONS

For microstructural engineering, it is important to have information on the actual volumetric grain size. The methods of Takayama *et al.*[7] as well as Matsuura and Itoh[8] were employed to estimate the spatial grain-size distribution from the measured 2-D one. Takayama's comparatively simple method is only applicable when the grain-size distribution is log normal, *i.e.*, normal growth is the dominant process. However, it yields similar results to those obtained by the more general and sophisticated method of Matsuura and Itoh. The Matsuura–Itoh method can be used for any type of grain-size distribution. Therefore, it offers the potential also to estimate the 3-D distributions of recrystallized grains as well as of ferrite grains resulting from austenite decomposition during cooling and coiling.

Austenite grain growth kinetics in Al-killed plain carbon steels depend strongly on the preheating schedule, which controls the degree of AlN precipitation, and its effect on grain-boundary movement. The effective pinning force can be estimated with the statistical grain growth model of Abbruzzese and Lücke. Significant pinning is confirmed for the experimental condition of reheating from room temperature, but austenite grain growth in a hot-strip mill before finishing can be expected to occur unpinned for plain carbon steels. Analytical expressions are proposed to predict austenite grain growth in low-carbon, plain carbon steels above 1000 °C. Further, it is concluded that during finish rolling, the austenite grain-size evolution is determined by recrystallization, and subsequent grain growth can be neglected. Consequently, further studies shall be focused on the determination of the recrystallized grain size.

Because of the fundamental character of the presented model for grain growth in plain carbon steels, this approach appears to be applicable to grain growth in any other metal or alloy as long as texture effects can be neglected. Employing the Abbruzzese–Lücke model, the pinning parameter can be determined from measurements of the grain growth kinetics. However, extreme caution has to be taken

when extrapolating laboratory data to industrial conditions since substantially different pinning forces may exist in both situations, as illustrated here for plain carbon steels.

NOMENCLATURE

A	mean grain area
b	magnitude of the Burgers vector
d_A	equivalent area diameter (EQAD)
$d_{A,0}$	initial equivalent area diameter
d_g	median grain size value of log normal distribution
d_m	average grain size of 3-D distribution
$d_{m,0}$	initial average grain size of 3-D distribution
d_V	mean volumetric grain size
D_{gb}	grain boundary diffusivity
$D_{o,gb}$	pre-exponential factor of grain boundary diffusivity
f	grain size distribution
f_i	fraction of grains of size i
F_{ij}	driving force for grain growth between grains of size i and j
F_P	pinning force
k	Boltzmann constant
K	grain growth constant
K_o	fitting parameter in grain growth power law
l	mean linear intercept
m	grain growth exponent
M_{gb}	grain boundary mobility
n	number of grain size classes
N_i	number of grains per unit volume in size class i
N_{tot}	total number of grains per unit volume
P	pinning parameter
Q	apparent activation energy of grain growth (power law)
Q_{gb}	activation energy of grain boundary diffusion
r	average particle radius
R	gas constant
R_i	radius of grain of size i
R_{lim}	limiting grain radius
s	standard deviation of log normal grain size distribution
s_0	initial standard deviation of log normal grain size distribution
t	time
T	temperature
w_{ij}	probability that grains i and j are neighbors
α	geometrical multiplying factor
γ_{gb}	grain boundary energy
ϕ	heating rate
φ	cooling rate
ν	volume fraction of precipitates

ACKNOWLEDGMENTS

The authors appreciate the financial support received from the American Iron and Steel Institute (AISI) and the Department of Energy (DOE). The assistance of B. Chau, who performed the Gleeble tests, is gratefully acknowledged.

REFERENCES

1. C.M. Sellars and J.A. Whiteman: *Met. Sci.*, 1979, vol. 13, pp. 187-94.
2. E. Anelli: *Iron Steel Inst. Jpn. Int.*, 1992, vol. 32, pp. 440-49.
3. P.D. Hodgson and R.K. Gibbs: *Iron Steel Inst. Jpn. Int.*, 1992, vol. 32, pp. 1329-38.
4. S. Licka and J. Wozniak: *Kov. Mater.*, 1982, vol. 20, p. 562.
5. T. Gladman and F.B. Pickering: *J. Iron Steel Inst.*, 1967, vol. 205, pp. 653-64.
6. J.P. Drolet and A. Galibois: *Metall. Trans.*, 1971, vol. 2, pp. 53-64.
7. Y. Takayama, N. Furushiro, T. Tozawa, H. Kato, and S. Hori: *Mater. Trans. JIM*, 1991, vol. 32, pp. 214-21.
8. K. Matsuura and Y. Itoh: *Mater. Trans. JIM*, 1991, vol. 32, pp. 1042-47.
9. G. Abbruzzese and K. Lücke: *Mater. Sci. Forum*, 1992, vols. 94–96, pp. 597-604.
10. E.B. Hawbolt and B. Chau: private communication to C. Devadas, Ph.D. Thesis, The University of British Columbia, Vancouver, 1989.
11. A. Giumelli: Master's Thesis, The University of British Columbia, Vancouver, 1995, p. 48.
12. *1994 Annual Book of ASTM Standards*, vol. 3.01, ASTM Standard Designation E112-88, ASTM, Philadelphia, PA, 1994, pp. 227-51.
13. S.A. Saltikov: *Stereology*, H. Elias, ed., Springer, New York NY, 1967, pp. 163-73.
14. K.P. Huang and W. Form: *Prakt. Met.*, 1990, vol. 27, pp. 332-40.
15. S.K. Kurtz and F.M.A. Carpay: *J. Appl. Phys.*, 1980, vol. 51, pp. 5725-44.
16. F.G. Wilson and T. Gladman: *Int. Mater. Rev.*, 1988, vol. 33, pp. 221-86.
17. J. Kunze: *Nitrogen and Carbon in Iron and Steel -Thermodynamics-*, Akademie-Verlag, Berlin, 1990, pp. 188-90.
18. W.C. Leslie, R.L. Rickett, C.L. Dotson, and C.S. Walton: *Trans. ASM*, 1954, vol. 46, pp. 1470-97.
19. N.A. Gjostein, H.A. Domian, H.I. Aaronson, and E. Eichen: *Acta Metall.*, 1966, vol. 14, pp. 1637-44.
20. H.J. Frost and M.F. Ashby: *Deformation-Mechanism Maps*, Pergamon Press, Oxford, United Kingdom, 1982, pp. 60-70.
21. C. Zener: private communication to C.S. Smith: *Trans. TMS-AIME*, 1948, vol. 175, p. 15.
22. G. Wang: Ph.D. Thesis, McGill University, Montreal, 1990.
23. J.E. Burke and D. Turnbull: *Progr. Met. Phys.*, 1952, vol. 3, pp. 220-92.
24. N. Komatsubara, K. Kunishige, S. Okaguchi, T. Hashimoto, K. Ohshima, and I. Tamura: *Sumitomo Search*, 1990, No. 44, pp. 159-68.
25. M.P. Anderson, G.S. Grest, and D.J. Srolovitz: *Phil. Mag. B*, 1989, vol. 59, pp. 293-329.
26. Y.L. Qian: *HSLA Steels: Processing, Properties and Applications*, G. Tither and S.H. Zhang, eds., TMS, Warrendale, PA, 1992, pp. 209-15.